34th Annual International Conference of the IEEE EMBS
San Diego, California USA, 28 August - 1 September, 2012

Electrical Impedance Tomography Reconstruction Through Simulated Annealing with Total Least Square Error as Objective Function

Thiago de Castro Martins and Marcos de Sales Guerra Tsuzuki

Abstract— **The EIT reconstruction problem can be solved as an optimization problem where the divergence between a simulated impedance domain and the observed one is minimized. This optimization problem can be solved by a combination of Simulated Annealing (SA) for optimization and Finite Element Method (FEM) for simulation of the impedance domain. This combination has usually a very high computational cost, since SA requires an elevated number of objective function evaluations and those, obtained through FEM, are often expansive enough to make the whole process inviable. In here it is presented a new approach for EIT image reconstructions using SA and partial evaluations of objective functions based on overdetermined linear systems. This new reconstruction approach is evaluated with experimental data and compared with previous approaches.**

I. Introduction

EIT is a diffuse imaging technique for determining the electrical conductivity distribution inside an object from its boundary measurements. A set of electrodes is attached to the object surface, for example, a human body, then electrical current is injected through these electrodes and electrical potential on these electrodes are measured. In EIT it is possible to reconstruct either difference or static images. The difference image modality can be used when changes in the resistivity occur [1]. The reconstruction of static image is a substantially more difficult problem than the difference imaging problem because it is necessary to have a reference voltage.

This paper is structured as follows. Section II presents the problem formulation. Section III explains the proposed algorithm where a SA with incomplete evaluation of the combined objective functions is used to solve the EIT reconstruction problem. In section IV some results obtained from physical data are presented. Finally, section V rounds up the paper with the conclusions.

II. Background

A. Formulation of the Forward Problem

The flow of electrical current within a conductive thin film, Ω, can be described at any point by the 2D Laplacian equation

$$\nabla(\sigma\nabla\phi) = 0 \tag{1}$$

where σ is the film conductivity and ϕ is the electrical potential. The typical *forward problem* in EIT is given the conductivity distribution σ and the current J injected through boundary electrodes, find the potential distribution ϕ within Ω and in particular the resulting potentials at the measurement electrodes ϕ_m. The frequencies used in EIT are low enough so that the quasi-static approximation holds, and thus one can ignore capacitive and inductive effects. At the boundary, currents are injected through electrodes; thus the current density J_l injected through the l-th electrode is given by (current pattern)

$$\sigma\frac{\partial\phi}{\partial\hat{n}} = J_l \tag{2}$$

where $\hat{n}$ is the external normal versor, and the current density is zero elsewhere at the boundary [2].

B. The Inverse Problem

The inverse problem is formulated as given the injected currents J_l and the potentials at measurement electrodes ϕ_m, find the electrical conductivity distribution σ within Ω. The Laplace equation (1) with Dirichlet and Neumann boundary conditions applied is referred to as the continuum model of the forward problem [3]. If considering only the real part of conductivity, the model is still valid with a unique and strictly positive conductivity function σ [4].

For an irregular domain and isotropic media, analytical solution to the Laplace equation (1) with boundary condition (2) is unknown; thus, the partial differential equations were approximated by the FEM, the domain is discretized with triangular linear elements with constant conductivity and both problems, forward and inverse, are solved numerically. The virtual potential principle associated with the Laplace equation provides the local element matrices. When the local element matrices are stated in terms of the global coordinates of the mesh, the global conductivity matrix [3] which includes electrode contact impedance effects, is obtained; then the following relation holds

$$K\cdot\Phi = C \tag{3}$$

where $K(\sigma)\in\mathbb{R}^{s\times s}$ is the conductivity matrix calculated at a given particular distribution σ, Φ is a matrix containing nodal potentials corresponding to each applied current pattern, and $\mathbf{C}$ represents p linearly independent current patterns.

III. Proposed Algorithm

One possible approach to the EIT inverse problem is to look at it as an optimization problem, where the optimization variables are parameters of a simulated domain and the objective function is some measure of consistency between the data obtained from the simulated domain and the measured

This work was supported by FAPESP (Grants 2009/07173–2 and 2010/19380–0). M. S. G. Tsuzuki was partially supported by CNPq (Grants 304.258/2007–5 and 309.570/2010–7). T. C. Martins and M. S. G. Tsuzuki are with Computational Geometry Laboratory, Escola Politécnica, São Paulo University, Brazil. thiago@usp.br.

data. Since, as seen in section II-B, the FEM can be used to solve the forward problem on a simulated domain, one possibility for such objective function is to take the Euclidean distance

$$E(\sigma) = \sqrt{\Sigma|\Phi_m^i - \Phi_c^i(\sigma)|_2} \tag{4}$$

between the measured electric potentials Φ_m^i and the calculated potentials $\Phi_c^i(\sigma)$ for every applied current pattern. Indeed, the minimization of (4) is a classic approach to EIT [5, 6, 7, 8]. In [5] it was pointed that the minimization of (4) using gradient-based algorithms is difficult, since (4) is often ill-conditioned. Herrera et al. [6] avoided the computation of objective function gradients by means of SA and by doing so, managed to reconstruct very accurate conductivity distributions of the body, but at a very high computational cost. This is unsurprising, as each step of the SA involves the solution of a full FEM problem in order to evaluate the objective function.

Martins et al. [7, 8] proposed a mitigation of this high computational cost: instead of fully evaluating the objective function E at each SA iteration, an estimate $\tilde{E}$ and upper and lower boundaries E_{max} and E_{min} are obtained. Since SA deals only with variations of the objective function between iterations, those are converted in an estimate and boundaries of variation $\Delta\tilde{E}$, ΔE_{max}, ΔE_{min}. It was shown if in a given iteration $\Delta\tilde{E}$, ΔE_{max}, ΔE_{min} satisfy

$$e^{-\Delta E_{max}/_{kt}} \geq \begin{cases} 1 - P_{err} & \text{if } \Delta\tilde{E} \leq 0, \\ e^{-\Delta\tilde{E}/_{kt}} - P_{err} & \text{if } \Delta\tilde{E} > 0 \end{cases} \tag{5}$$

$$e^{-\Delta E_{min}/_{kt}} \leq min(1, P_{err} + e^{-\Delta\tilde{E}/_{kt}}) \tag{6}$$

then the probability of SA at that iteration deviating of an SA with full objective function evaluation is less than P_{err}. Estimates of the objective function were obtained by iteratively solving (3) with Conjugated Gradients (CG) algorithm while obtaining an upper limit on the norm of the error at each CG iteration using a technique described in [9]. In order to convert limits on norms of the error on solutions of (3) to limits on the error on the evaluation of (4), the following simplifications were adopted:

1) The CG error norm limit at iteration i is taken as the error norm limit at iteration $i+d$, that is, the error limit for a given iteration is only obtained d iterations latter, where d is a parameter linked to the conditioning of the matrix (in [7] $d = 1$ was used). This is correct as the CG error norm is monotonically decreasing.
2) The error norm limit for all combined variables (potentials at the mesh nodes) is taken as the error norm limit for just the electrode potentials.
3) The sum of the squares of the error norm limits for all current patterns is taken as the limit for the squared norm of the objective function error (correct by triangular inequality).

Each of those simplifications leads successively to an error overestimation. Simplification 2 is problematic, as it does not scale well with mesh density. Indeed, as the mesh density increases, the relation between the number of electrodes and the number of nodes decrease, leading to increasingly the error norm overestimation. As such, it would be advantageous to obtain a method that scales with increased mesh density.

A. Least squares error as an objective function

By taking (3), reordering the variables such that the electrode potentials correspond to the last elements of Φ, one can write

$$\begin{pmatrix} K_{ii} & K_{ic}^T \\ K_{ic} & K_{cc} \end{pmatrix} \begin{pmatrix} \Phi_i \\ \Phi_c \end{pmatrix} = \begin{pmatrix} 0 \\ J_l \end{pmatrix} \tag{7}$$

where Φ_i is the vector of tensions at the internal nodes, Φ_c is the vector of tensions at the electrodes, K_{ii}, K_{ic} and K_{cc} are blocks of the matrix $K(\sigma)$. Considering $\Phi_c = \Phi_m$ (that is, the potentials at electrodes of the simulated domain are identical to the measured ones) and allowing an error on (7), then

$$\hat{K}(\sigma)\Phi + \mathbf{e} = \hat{\mathbf{J}}_\mathbf{l} \tag{8}$$

where

$$\hat{K} = \begin{pmatrix} K_{ii} \\ K_{ic} \end{pmatrix} \quad \hat{J}_l = \begin{pmatrix} -K_{ic}^T \Phi_m \\ J_l - K_{cc}\Phi_m \end{pmatrix} \tag{9}$$

and $\mathbf{e}$ is an error vector added to the reduced system to make it consistent with the replacement $\Phi_c \Rightarrow \Phi_m$. Since the error required tends to zero as Φ_c approaches Φ_m, one could take its minimum, subject to (8), as the measure of consistency between the simulated domain and the physical experiment for a given current pattern. A new objective function is

$$E(\sigma) = \sqrt{\sum_l D^l(\sigma)^2} \tag{10}$$

$$D^l = \min_\Phi \left\{ \sqrt{\mathbf{e^T e}} : \hat{K}(\sigma)\Phi + \mathbf{e} = \hat{\mathbf{J}}_\mathbf{l} \right\} \tag{11}$$

The minimization problem in (11) is a typical least squares problem which solution is given by

$$D^{l\,2} = \hat{J}_l^T \hat{J}_l - \hat{J}_k^T \hat{K} \left(\hat{K}^T \hat{K}\right)^{-1} \hat{K}^T \hat{J}_l. \tag{12}$$

In [11, chap. 7], Golub exploited the link between the Lanczos tridiagonalization algorithm and Gaussian Quadrature to estimate efficiently the values of quadratic forms $v^T f(A) v$ where v is a vector, A is a symmetric matrix and $f(x)$ is an analytical function. The Lanczos Algorithm [12] is a decomposition algorithm that for a given symmetric positive definite matrix A iteratively construct tridiagonal matrices L_k such that

$$\mathbf{A}\mathbf{V}_k = \mathbf{V}_k \cdot \mathbf{T}_k + \eta_k v_{k+1} (e_k)^T \tag{13}$$

where $\mathbf{V}$ is an orthonormal matrix and $\mathbf{T}$ is a tridiagonal symmetric matrix.

The form $v^T f(A) v$ can be expressed as a Riemman-Stieltjes integral $\int_a^b f(\lambda)\, \mathrm{d}\alpha(\lambda)$ for a specific measure $\alpha(\lambda)$ obtained from v and the spectral decomposition of A (the integration limits are the lowest and highest eigenvalues of A). That integral can be in turn approached by Gaussian Quadrature rules whose coefficient are directly obtained from

the $\mathbf{T}_k$ matrices from Lanczos algorithm when its starting vector is v. Indeed, for a Gauss rule,

$$v^T f(A)\, v = \|v\|^2 f(T_k)_{1,1} + \varepsilon_k = \|v\|^2 g_k + \varepsilon_k \qquad (14)$$

and for a Gauss-Radau rule, the estimate is

$$v^T f(A)\, v = \|v\|^2 f\left(\tilde{T}_k\right)_{1,1} + \tilde{\varepsilon}_k = \|v\|^2 \tilde{g}_k + \tilde{\varepsilon}_k \qquad (15)$$

where $\tilde{T}_k$ is a modification of the matrix T_k in order to add to its eigenvalues the lowest eigenvalue of A.

In particular, for $f(x) = x^{-1}$, ε_k is positive and monotonically decreasing with k while $\tilde{\varepsilon}_k$ is negative and monotonically decreasing. As such, $\|v\|^2 g_k$ and $\|v\|^2 \tilde{g}_k$ create sequences of increasingly tighter lower and upper boundaries for $v^T f(A)\, v$ (it can be shown that in exact arithmetic, $g_n = \tilde{g}_n = {}^{v^T f(A) v}/_{\|v\|^2}$, where n is the rank of A). One can thus iteratively obtain boundaries for the values of (12) (in this case, Gauss rule gives an upper boundary and Gauss-Radau rule gives a lower boundary). Conditions (5) and (6) can be used as Lanczos algorithm iterations stopping criteria.

While the Lanczos algorithm could be applied directly by taking $A = \hat{K}^T \hat{K}$, in [13] it is proposed a variation called "Lanczos bidiagonalization II" that takes advantage of the special nature of $\hat{K}^T \hat{K}$. The algorithm is as follows (adapted from [13]):

$$\begin{array}{c} \mathbf{r}_0 = \hat{J}, \delta_0 = \|\mathbf{r}_0\|, \mathbf{p}_0 = {}^{\mathbf{r}_0}/_{\delta_0}, \mathbf{u}_0 = \hat{K}^T p_0 \\ \gamma_k = \|\mathbf{u}_{k-1}\|, \mathbf{q}_k = {}^{\mathbf{u}_k}/_{\gamma_{k+1}}, \delta_k = \|\mathbf{r}_k\| \\ \mathbf{p}_k = {}^{\mathbf{r}_k}/_{\delta_k}, \mathbf{u}_k = \hat{K}^T p_{k-1} - \delta_{k-1}\mathbf{q}_{k-2} \\ \mathbf{r}_k = \hat{K}\mathbf{q}_{k-1} - \gamma_i \mathbf{p}_{k-1} \end{array} . \qquad (16)$$

The algorithm that builds matrices

$$C_k = \begin{pmatrix} \lambda_1 & & \\ \delta_1 & \ddots & \\ & \ddots & \gamma_k \\ & & \delta_k \end{pmatrix} \qquad (17)$$

. The Gauss rule estimate of ${D^l}^2$ is given by $\|\hat{J}_l\| - \|\hat{K}\hat{J}_l\| g_k$, $g_k = \left({C_k}^T C_k\right)^{-1}_{1,1}$. To obtain this last value, a QR factorization such that ${C_k}^T C_k = {B_k}^T B_k$ is used,

$$B_k = \begin{pmatrix} \phi_1 & \psi_1 & & \\ & \ddots & \ddots & \\ & & \phi_{k-1} & \psi_{k-1} \\ & & & \phi_k \end{pmatrix} \qquad (18)$$

Finally, $({B_k}^T B_k)^{-1}_{1,1}$ can be obtained by inspection. The relevant iterations to obtain g_k are:

$$\begin{array}{c} {\phi_1}^2 = {\gamma_1}^2 + {\delta_1}^2, c_1 = {}^{-\gamma_1}/_{\phi_1}, \pi_1 = {}^{1}/_{{\phi_1}^2}, g_0 = 0 \\ {\phi_k}^2 = {c_{k-1}}^2 {\gamma_k}^2 + {\delta_k}^2, s_k = {}^{\delta_k}/_{\phi_k} \\ c_k = -c_{k-1}{}^{\gamma_k}/_{\phi_k}, \psi_k = s_i \gamma_{k+1} \\ \pi_k = \pi_{k-1} {\psi_{k-1}}^2 / {\phi_k}^2, g_k = g_{k-1} + \pi_k \end{array} . \qquad (19)$$

For the Gauss-Radau rule, matrix $\tilde{T}_k = \tilde{B}_k^T \tilde{B}_k$ must be constructed from T_k so that it has the lowest eigenvalue of $\hat{K}^T \hat{K}$. One can show that this is equivalent to a simple modification on ϕ_k, the last element of B_k. For that, first the components of T_k must be computed. If α_k and β_k are the diagonal and subdiagonals respectively,

$$\alpha_k = \gamma_k^2 + \delta_k^2, \quad \beta_k = \gamma_{k+1}\delta_k \qquad (20)$$

if a is the lowest eigenvalue of $\hat{K}^T \hat{K}$, the iterations for calculating $\tilde{g}_k$ are:

$$\begin{array}{c} \tilde{\alpha}_1 = a, \tilde{d}_1 = \alpha_1 - a \\ \tilde{d}_k = \alpha_k - a - {}^{\beta_{k-1}^2}/_{\tilde{d}_{k-1}}, \tilde{\alpha}_k = a + {}^{\beta_{k-1}^2}/_{\tilde{d}_{k-1}} \\ \tilde{\phi}_k^2 = \tilde{\alpha}_k - \psi_{k-1}^2, \tilde{g}_k = g_k + \pi_k \psi_k^2 / \tilde{\phi}_{k+1}^2 \end{array} . \qquad (21)$$

Of course, there remains the problem of obtaining the lowest eigenvalue of $\hat{K}^T \hat{K}$. In [11, chap. 12] there is a suggestion of using the extreme eigenvalues of T_k as approximations for the extreme eigenvalues of $\hat{K}^T \hat{K}$. Since a LLT factorization of T_k is obtained as a byproduct of the iterations in (19), a reverse power iteration can be easily performed to obtain a good estimate of a. In practice, for a good estimate of a much more iterations are needed (here it is used $n/8$, where n is the rank of $\hat{K}^T \hat{K}$) than the required by conditions (5) and (6). This is not too wasteful though, as those iterations can be performed while solving for a single current pattern and then the a value can be reused while solving for every other current pattern.

Just like in [7], one can also apply preconditioning to this technique and reuse values from previous SA iterations as initial guesses in order to improve convergence.

B. Shortcomings and Workarounds

Since SA can change the elements of matrix $\hat{K}$, it can make the subproblem of optimizing (11) arbitrarily ill-conditioned by making K_{ic} very close to zero. Physically, this is the equivalent of creating a domain with an outer ring of very low conductance. Under those circumstances, arbitrarily low values of (12) can be obtained. One possible solution to this problem is to impose a fixed value of conductance on the outer layer of the domain, thus fixing K_{ic}. It is very convenient, because the reconstruction procedure proposed in [7, 8] is able to find the impedance of the outer layers very early in the process. One can then start the reconstruction using the procedure in [7], stop it when the outer impedance has converged and use its data to fix K_{ic}. This has the added benefits of reducing the optimization variables of the algorithm (although this benefit is of marginal importance - the inner layers correspond to almost all impedance parameters of the problem) and fixing $\hat{J}_l$ between SA iterations (since $\hat{J}_l$ do not depend on K_{ii}).

IV. Results

To validate the proposed approach, the experiment in [7, 8] was reproduced, with three cucumber slices immersed in a cylindrical container with 32 electrodes (see Fig. 2a). The same 32 linearly-independent current patterns were applied. The image was reconstructed both with the process proposed in [7, 8] and the process proposed here. The same SA parameters were used for both reconstructions, except the initial temperature, which was reduced tenfold to account

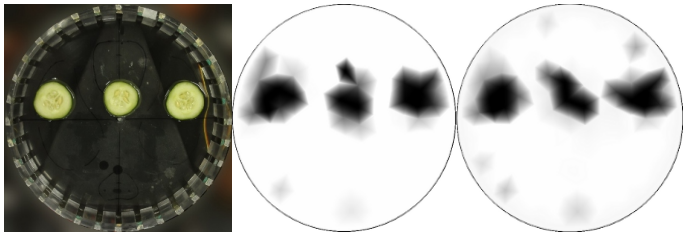

(a) (b) (c)

Fig. 1: (a) "Line" Phantom and its reconstructions using (b) the approach in [8] and (c) the new approach.

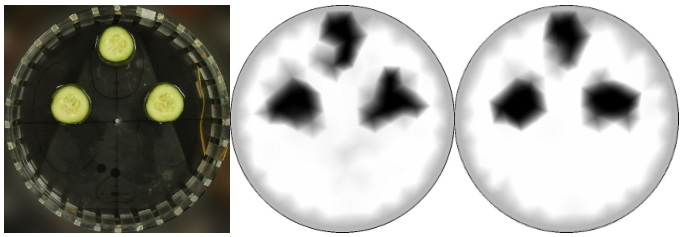

(a) (b) (c)

Fig. 2: (a) "Triangle" Phantom and its reconstructions using (b) the approach in [8] and (c) the new approach.

for the different scale of the objective function of the new process.

Two patterns of cucumber slices were tested, one where the slices were arranged in a triangular pattern (see Fig. 2a and its reconstructions in Fig. 2b and 2c) and another one where the slices were arranged in line (see Fig. 1a and its reconstructions in Fig. 1b and 1c).

One can see that the image reconstructed with the new process is as good as the obtained with the old one. The few impedance artifacts seen in the outer layers (particularly in Fig 1c) can be explained by the greater sensitivity of this process to mesh errors (a coarse mesh tends to underestimate electrode impedance). This greater sensitivity is related to the fact that the new process impose $\Phi_c = \Phi_m$ and the conductivity of the outer layer is obtained from the old process, that tolerate differences between Φ_c and Φ_m. It is expected that with a denser mesh, those artifacts would go away.

On the performance front, the number of iterations required to evaluate the objective function on the new algorithm is on average less than $1/3$ of the required by the old one. Considering that each iteration of the new algorithm is roughly twice as costly as an iteration of the old one, this means a speedup factor of about $3/2$.

V. Conclusions and Future Work

It is proposed here a new approach to solve the EIT inverse problem that mitigates the scalability problems identified in [7, 8]. This approach uses estimates with bounded error on the solution of least square problems and a variation of SA that deals with incomplete evaluation of objective functions. Initial results show that the new approach has potential of a greater performance than the reconstruction process proposed in [7, 8]. One of the process limitations is that, due to potential ill-conditioning of the underlying least square problems, it is unable to calculate the impedance distribution on the outer layer of the domain. It would be interesting to verify how regularization techniques such as Tikhonov regularization can eliminate this limitation.

References

[1] D. C. Barber and B. H. Brown, "Applied potencial tomography," *J Phys E Sci Instrum*, 17, 723–733, 1984.

[2] B. H. Brown and A. Seagar, "The sheffield data collection system," *Clin Phys Physiol M*, 8, A91–A97, 1987.

[3] F. C. Trigo, R. G. Lima, and M. B. P. Amato, "Electrical impedance tomography using the extended Kalman filter," *IEEE T Bio Med Eng*, 51, 72–81, 2004.

[4] R. V. Kohn and M. Vogelius, "Determining conductivity by boundary measurements II. interior results," *Commun Pur Appl Math*, 38, 643–667, 1985.

[5] L. A. M. Mello, C. R. de Lima, M. B. P. Amato, R. G. Lima, and E. C. N. Silva, "Three-dimensional electrical impedance tomography: a topology optimization approach." *IEEE T Bio Med Eng*, 55, 531–40, 2008.

[6] C. N. L. Herrera, M. F. M. Vallejo, F. S. Moura, J. C. C. Aya, and R. G. Lima, "Electrical impedance tomography algorithm using simulated annealing search method," in *Proc Int Cong Mech Eng*. Brasília, Brazil, 2007.

[7] T. C. Martins, E. D. L. B. Camargo, R. G. Lima, M. B. P. Amato, and M. S. G. Tsuzuki, "Electrical impedance tomography reconstruction through simulated annealing with incomplete evaluation of the objective function." in *Proc 33rd Annual Int Conf IEEE EMBS*. Boston, USA, 2011.

[8] T. C. Martins, E. D. L. B. Camargo, R. G. Lima, M. B. P. Amato, and M. S. G. Tsuzuki, "Image reconstruction using interval simulated annealing in electrical impedance tomography," *IEEE T Bio Med Eng*, 10.1109/TBME.2012.2188398.

[9] G. Meurant, "Estimates of the l2 norm of the error in the conjugate gradient algorithm," *Numer Algorithms*, 40, 157–169, 2005.

[10] G. H. Golub and G. Meurant, "Matrices, moments and quadrature", in *Numerical Analysis*, D. F. Griffiths and G. A. Watson Eds., 1994, 303, 105–156.

[11] G. H. Golub and G. Meurant, *Matrices, Moments and Quadrature with Applications*, Princeton University Press, 2010.

[12] G. Meurant, *The Lanczos and conjugate gradient algorithms: from theory to finite precision computations*, SIAM, 2006.

[13] G. H. Golub, U. v. Matt, "Generalized cross-validation for large scale problems," *J Comput Graph Stat*, 6, 1–34, 1995.